

iScience, Volume 25

Supplemental information

Structural and functional properties of spinal dorsal horn neurons after peripheral nerve injury change overtime via astrocyte activation

**Miyuki Kurabe, Mika Sasaki, Kenta Furutani, Hidemasa Furue, Yoshinori
Kamiya, and Hiroshi Baba**

Supplemental information

Structural and functional Properties of Spinal Dorsal Horn Neurons after Peripheral Nerve Injury Change over Time via Astrocyte Activation

Miyuki Kurabe¹, Mika Sasaki, Kenta Furutani, Hidemasa Furue, Yoshinori Kamiya, and Hiroshi Baba

Figure S1

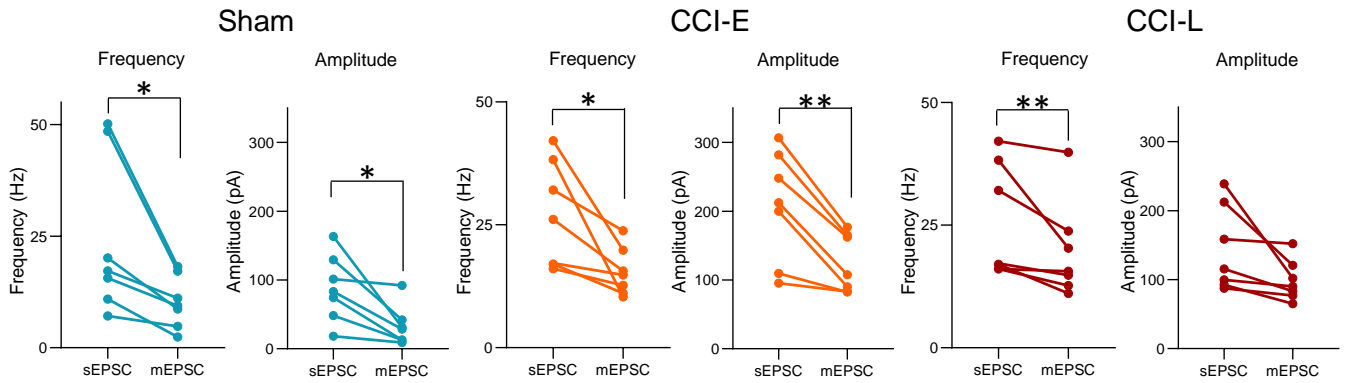


Figure S1. miniature EPSCs. Related Figure 3.

Changes in EPSCs before and after perfusion of TTX (0.5 μ M) to the spinal surface.

Sham ($n = 7$ cells from 4 rats); Frequency: before 24.23 ± 6.68 Hz, after 10.25 ± 2.22 Hz, * $P = 0.0244$, Amplitude: before 88.26 ± 18.40 pA, after 32.68 ± 10.87 pA, * $P = 0.0155$.

b, CCI-E ($n = 7$ cells from 4 rats); Frequency: before 44.23 ± 5.05 Hz, after 24.56 ± 2.56 Hz, ** $P = 0.0022$, Amplitude: before 207.7 ± 30.55 pA, after 124.0 ± 15.98 pA, *** $P < 0.0029$.

c, CCI-L ($n = 6$ cells from 4 rats); Frequency: before 26.98 ± 4.07 Hz, after 15.45 ± 1.84 Hz, * $P = 0.0208$, Amplitude: before 143.7 ± 23.15 pA, after 98.60 ± 11.21 pA, $P = 0.0543$

Significant differences were assessed by paired t-test. Data are presented as means \pm s.e.m.

Figure S2

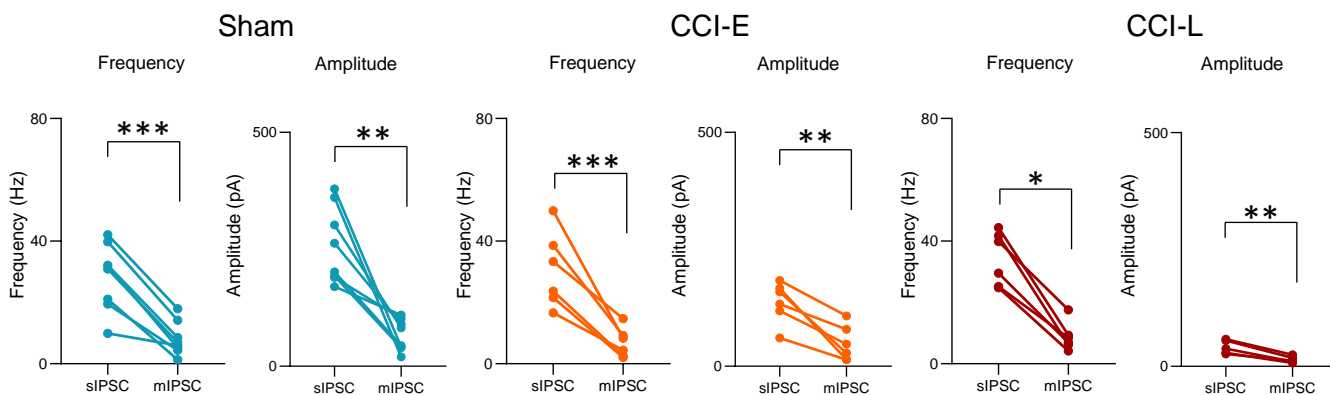


Figure S2. miniature IPSCs. Related Figure 4.

Changes in IPSCs before and after perfusion of TTX (0.5 μ M) to the spinal surface.

a, Sham ($n = 8$ cells from 5 rats); Frequency: before 28.43 ± 3.85 Hz, after 8.07 ± 1.93 Hz, ***P=0.0001, Amplitude: before 257.5 ± 28.95 pA, after 66.17 ± 11.90 pA, **P = 0.0012.

b, CCI-E ($n = 7$ cells from 4 rats); Frequency: before 44.23 ± 5.05 Hz, after 24.56 ± 2.56 Hz, **P = 0.0022, Amplitude: before 136.8 ± 18.01 pA, after 48.20 ± 15.47 pA, **P = 0.0039

c, CCI-L ($n = 6$ cells from 4 rats); Frequency: before 26.98 ± 4.07 Hz, after 15.45 ± 1.84 Hz, *P = 0.0208, Amplitude: before 41.32 ± 6.53 pA, after 14.54 ± 3.10 pA, **P = 0.0028.

Significant differences were assessed by paired t-test. Data are presented as means \pm s.e.m.

Figure S3

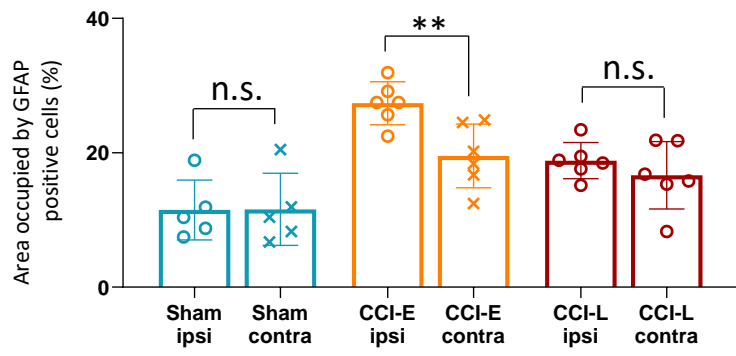
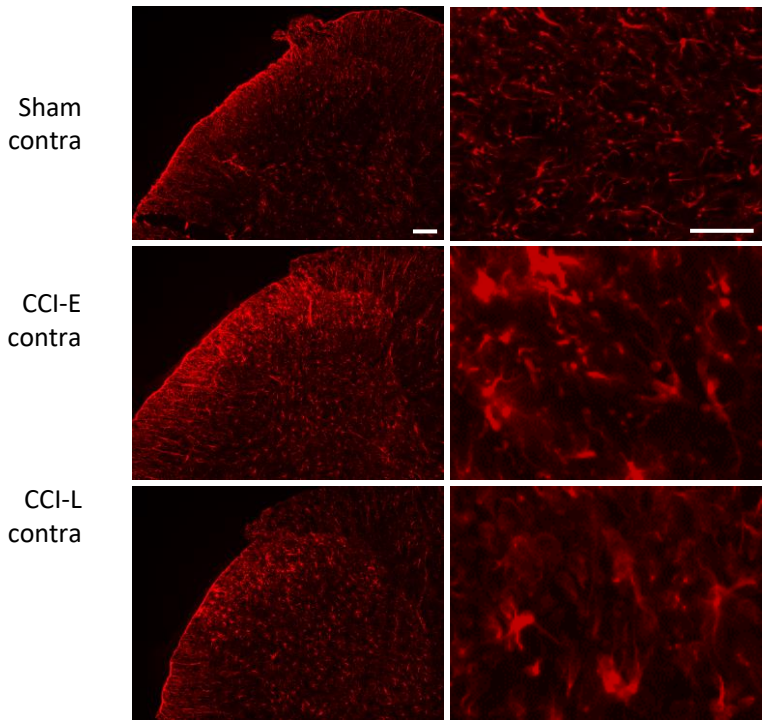


Figure S3. Comparison of ipsilateral and contralateral astrocyte upregulation in SDH after CCI. Related Figure 5.

(A) Low and high magnification images of GFAP-positive cells in contralateral SDH of Sham, CCI-E, and CCI-L rats. Scale bars are 100 μ m (left panels) and 50 μ m (right panels). (B) GFAP quantification. The percentage area occupied by GFAP positive cells in the SDH was analysed. Histograms indicate the relative mean area occupied by GFAP-positive cells on the ipsilateral and contralateral sides of the SDH in Sham, CCI-E, and CCI-L rats. (Sham-ipsi: 11.48 ± 1.99 %, Sham-contra: 11.57 ± 2.40 %, $P = 0.978$; CCI-E-ipsi: 27.37 ± 1.30 %, CCI-E-contra: 11.57 ± 2.05 %, $**P = 0.0073$; CCI-L-ipsi: 18.83 ± 1.10 %, CCI-L-contra: 16.65 ± 2.40 %, $P = 0.3716$; $n = 5$ rats in Sham group, and $n = 6$ rats in CCI-E and CCI-L group respectively). Significant differences were assessed by two-sided unpaired Student's test. Data are presented as means \pm s.e.m. n.s., not significant.